Short-term facilitation of microbial litter decomposition by ultraviolet radiation

Yang Lin[1, 2*], Steven D. Karlen[3], John Ralph[3, 4], and Jennifer Y. King[1]

[1] Department of Geography, University of California, Santa Barbara, CA 93106, USA

[2] Department of Environmental Science, Policy, and Management, University of California, Berkeley, CA 94720, USA

[3] U.S. Department of Energy (DOE) Great Lakes Bioenergy Research Center, The Wisconsin Energy Institute, University of Wisconsin-Madison, Madison, WI 53726, USA

[4] Department of Biochemistry, University of Wisconsin-Madison, Madison, WI 53706, USA

[*]Corresponding author: ylin@ucsb.edu
Department of Environmental Science, Policy, and Management
130 Mulford Hall #3114
University of California, Berkeley, CA 94720

Abstract

Solar radiation plays an important role in carbon cycling by increasing the decomposition rates of plant litter and soil organic matter (i.e. photodegradation). Previous work suggests that exposure to radiation can facilitate microbial decomposition of litter by altering litter chemistry and consequently litter degradability (i.e. photopriming). However, it remains unclear to what extent photopriming contributes to litter decomposition processes and on what timescale photopriming operates. We conducted laboratory experiments to compare the effects of UV photopriming at two temporal scales (months versus days). In one experiment, we found that four months of UV exposure induced a significant but small (3-4%) mass loss in two of three litter species commonly found in California oak savanna; however, UV exposure did not alter litter degradability as measured by microbial respiration in an incubation experiment. We also found that UV exposure had limited effects on lignin and other cell wall structures, but one month of microbial decomposition (in absence of UV exposure) significantly reduced lignin β-aryl ether inter-unit linkages and acetylated xylans. These results indicate that abiotic photodegradation alone was ineffective at breaking down lignin. In another experiment, litter of a common grass was exposed to either alternating UV radiation and dark conditions, or constant darkness for 128 days. We found that the alternating UV exposure increased litter CO_2 production in both dark and UV phases over that observed in constant darkness. This led to a 35% greater release of CO_2 from the alternating UV exposure treatment between days 65 and 128 of the experiment. These results demonstrate that alternating UV exposure with dark conditions is key to enabling photopriming on a timescale of days. Overall, we identify short-term photopriming as a novel mechanism behind photodegradation. Our results also challenge the conventional hypothesis that abiotic processes are primarily responsible for degrading lignin during photodegradation.

Keywords

39 Photo-oxidation; photodegradation; cellulose; hemicellulose; NMR (nuclear magnetic resonance);
40 HSQC (heteronuclear single-quantum coherence)

41

1. Introduction

There are large uncertainties in current predictions of how the terrestrial carbon (C) cycle will respond to future climatic changes (Smith et al., 2013; Carvalhais et al., 2014; Smith et al., 2016). A major source of uncertainty is the difficulty in quantifying ecosystem C fluxes and attributing their variations among abiotic and biotic controls (Lombardozzi et al., 2015; Wieder et al., 2015). Litter decomposition is the central ecosystem process that transfers C from a transient pool in vegetation to a stabilized pool in soil (Berg and McClaugherty, 2008). Conventional theories of litter decomposition focus on understanding the environmental and chemical controls of biotic decomposition (Melillo et al., 1982; Coŭteaux et al., 1995). Empirical models developed based on these theories are successful overall, but they systematically underestimate litter decomposition rates in many arid and semi-arid environments (Schaefer et al., 1985; Parton et al., 2007; Adair et al., 2008). This knowledge gap has sparked a new and growing field of research on photodegradation (Austin and Vivanco, 2006; King et al., 2012; Song et al., 2013; Liu et al., 2014; Barnes et al., 2015). Here, the term “photodegradation” refers to the combination of abiotic and biotic effects of solar radiation on decomposition processes.

Abiotic photodegradation refers to the photochemical and/or thermal mineralization of organic matter upon exposure to solar radiation, including ultraviolet (UV; 280-400 nm) and photosynthetically active radiation (PAR; 400-700 nm) (Brandt et al., 2009; Lee et al., 2012; Whelan and Rhew, 2014). Laboratory studies have linked abiotic photodegradation processes to the breakdown of litter and soil organic matter and emissions of CO, CO_2, CH_4, and volatile organic compounds (Schade et al., 1999; Leff and Fierer, 2008; Brandt et al., 2009). These abiotic emissions of trace gases are typically small in magnitude (reviewed by King et al., 2012), making it difficult to directly measure them in the field (van Asperen et al., 2015). The litter mass loss induced by abiotic photodegradation is also generally small (reviewed by Song et al., 2013; Wang et al., 2015) compared to the results from field studies showing that exposure to solar radiation

increased mass loss by 25% to 60% (Austin and Vivanco, 2006; Brandt et al., 2010; Huang et al., 2017).

Photodegradation can also contribute to litter mass loss by facilitating microbial decomposition, a process known as photopriming (Barnes et al., 2015). Photopriming has often been included as a key component of photodegradation (e.g., Day et al., 2007; Gallo et al., 2009). More recent studies have begun to isolate and quantify the specific contribution of photopriming to litter decomposition (Foereid et al., 2010; Lin et al., 2015b; Wang et al., 2015; Yanni et al., 2015; Austin et al., 2016). It is hypothesized that photopriming is enabled via abiotic photodegradation of lignin, a main component of the plant cell wall that usually impedes microbial decomposition (King et al., 2012; Baker and Allison, 2015). Degradation of lignin allows microbial decomposers to access other litter substrates, thus increasing microbial litter decomposition. Many studies support this mechanism and report radiation-induced decreases in litter lignin content and increases in litter degradability during microbial decomposition (Henry et al., 2008; Austin and Ballaré, 2010; Frouz et al., 2011; Wang et al., 2015; Austin et al., 2016). However, it is unclear whether the loss of lignin was caused solely by abiotic photodegradation or a combination of abiotic photodegradation and photopriming of microbial decomposition. In addition, a large number of studies did not find facilitation effects of radiation exposure on litter degradability, further questioning the prevalence of photopriming (Brandt et al., 2009; Kirschbaum et al., 2011; Lambie et al., 2014; Lin et al., 2015b).

Identifying the underlying mechanisms of photopriming would help to resolve the above contradicting results of photopriming research. Past photopriming studies usually separated radiation treatment and the assessment of litter degradability into two consecutive phases. The first phase, radiation treatment, typically lasted for several months to a year and was often implemented under field or greenhouse conditions (Henry et al., 2008; Lin et al., 2015b; Wang et al., 2015; Austin et al., 2016). The second phase, assessment of litter degradability, was generally

conducted without radiation manipulation under controlled field or laboratory conditions (Brandt et al., 2009; Lambie et al., 2014; Yanni et al., 2015; Austin et al., 2016). However, under natural conditions, litter experiences abiotic photodegradation and microbial decomposition simultaneously on a daily basis. Gliksman et al. (2016) recently demonstrated that daytime photodegradation primed litter microbial decomposition at night in a Mediterranean ecosystem, suggesting photopriming can occur at a diel scale. Therefore, photopriming might have occurred but was undetected during the first phase of a two-phase experiment. The two-phase design is thus likely to underestimate or misrepresent the contribution of photopriming to litter decomposition in the field. A comparison of the photopriming effects at different temporal scales (e.g. seasonal vs. daily) is currently lacking and would improve our understanding of the role of photopriming in litter decomposition processes.

Unlike the studies mentioned above, a number of other studies did not find preferential breakdown of lignin by photodegradation (Brandt et al., 2007; Lin and King, 2014; Baker and Allison, 2015), highlighting the lack of understanding of the underlying chemical mechanism behind photodegradation. Most previous studies relied on proximate analyses that sequentially extracted litter with solvents and assumed the acid-unhydrolyzable residues to be lignin. This assumption is strongly challenged in the field of decomposition science (Sluiter et al., 2010; Preston and Trofymow, 2015), which has led to several recent studies that examined changes in lignin chemical composition during photodegradation (Feng et al., 2011; Frouz et al., 2011). For instance, using two-dimensional nuclear magnetic resonance (2D NMR) spectroscopic techniques, we found that field UV radiation exposure degraded lignin β-aryl ether units and hemicelluloses (Lin et al., 2015a). In the current literature, however, there is no consistent pattern to describe how photodegradation alters lignin chemistry. It is also unclear whether abiotic photodegradation and microbial decomposition target similar lignin structures.

Here we present results from two controlled laboratory experiments that examine the mechanisms of photopriming at two different temporal scales. In the first experiment (*two-phase photopriming*), we exposed three types of litter to UV radiation for four months in the laboratory and evaluated the effects of abiotic photodegradation induced by UV radiation (hereafter, abiotic UV photodegradation) on litter mass loss and litter degradability. We also compared the effects of abiotic UV photodegradation and microbial decomposition on litter cell wall chemistry using 2D NMR techniques. In the second experiment (*short-term photopriming*), a grass litter was exposed to either alternating UV radiation and dark conditions or kept continuously in darkness in order to assess photopriming on a daily temporal scale. We hypothesized that 1) an extended period of UV exposure would stimulate litter mass loss due to abiotic photodegradation and increase litter biodegradability as a result of UV-induced lignin degradation; 2) abiotic UV photodegradation would be more effective in altering lignin chemistry compared to microbial decomposition; and 3) microbial decomposition of litter would be enhanced under an alternating light regime compared to continuous darkness as a result of short-term photopriming.

2. Materials and Methods

2.1. Study site and sample collection

Litter and soil samples were collected from the University of California's Sedgwick Reserve in Santa Ynez, CA, USA (34°42'N, 120°2'W), where the mean elevation is approximately 400 m.a.s.l., the mean annual precipitation is 380 mm, and the mean annual temperature is 16.8 °C. The study site features a Mediterranean climate with hot, dry summers and cool, wet winters. Vegetation is characteristic of a California oak savanna that is dominated by several invasive annual grass species: *Bromus diandrus*, *Avena fatua*, and *Bromus hordaceous*. Several oak species, including blue oak (*Quercus douglasii*), coast live oak (*Quercus agrifolia*), and valley

oak (*Quercus lobata*), are widely spaced in the grassland matrix. Soil is classified as Haploxerolls with high clay concentrations.

Standing dead, senesced litter from *B. diandrus* and *A. fatua* was harvested in July 2013 after the end of the growing season. Recently fallen leaves of *Q. douglasii* were also collected. Upon return to the laboratory, *B. diandrus* and *A. fatua* litter was cut into pieces of approximately 10 cm in length. All litter samples were oven-dried at 60 °C for two days and then stored in the dark at room temperature until used in the two experiments described here.

2.2. Two-phase photopriming experiment

Radiation exposure. The experiment follows a factorial design of litter type (*A. fatua*, *B. diandrus*, and *Q. douglasii*) and UV manipulation (UV exposure and control) with three replicates. Oven-dried litter was enclosed in custom-built envelopes that were made of UV-transparent polychlorotrifluoroethylene film (0.0635 mm thickness, HydroBlock GP2500, Honeywell International Inc., Morris Plains, NJ) and sealed on the edges with vinyl tape. This film is optically equivalent to Aclar film (Day et al., 2007; Uselman et al., 2011) and transmits over 94% of radiation in the UV range. By flipping the envelopes every week, both sides of the samples were exposed to UV radiation. Envelopes also helped to reduce overlapping of litter. Note that the envelopes were not air-tight. Eighteen envelopes were constructed. A set of three envelopes, each with one litter type, was placed 10 cm under four UV lamps (UVB-313EL, Q-Lab, Cleveland, OH) on a shelf in an environmental control room and irradiated continuously for four months ("UV exposure" treatment). The locations of three envelopes on the same shelf were rearranged every week to account for slight spatial variability in radiation intensity under the UV lamps. Three shelves were constructed to treat a total of 9 envelopes. Shelves were separated from each other with black stage curtain. A broadband radiometer with two sensors (UV-X, UV Products, Upland, CA) was used to monitor the UV radiation intensity that samples received in the UV-A and UV-B ranges. The UV-A sensor was calibrated to measure UV radiation centered

at 365 nm with a response curve ranging from 300 to 400 nm. The UV-B sensor was calibrated to measure UV radiation centered at 310 nm with a response curve encompassing 260 to 370 nm. Factory calibration of the UV sensors is traceable to the National Institute of Standards and Technology (NIST). The dose of UV radiation is comparable to that from past laboratory studies (Brandt et al., 2009; Lambie et al., 2014; van Asperen et al., 2015; see Results for details). The UV lamps were pre-burned for five days to stabilize radiation output. Radiation intensity was monitored periodically with the broadband radiometer, and no significant change was detected during the experiment. Note that UV lamps did emit a small amount of radiation in the visible and UV-C (< 280 nm, known to kill or inactivate microbes) ranges, which was assumed to have minor impacts on decomposition processes. The other 9 envelopes were kept in the dark inside a cardboard box in the same environmental control room ("control" treatment). Room temperature was cycled between 21 and 29 °C every 12 h. After the treatments, litter samples were dried in the oven at 60 °C, weighed to assess mass loss, and ground with a Wiley mill (Thomas Scientific, Swedesboro, NJ) through a standard US #20 mesh screen for further analyses.

Litter chemistry. For 2D NMR analyses, we included the 18 samples exposed to UV exposure and control treatments in the experiment above. To compare the effects of abiotic UV photodegradation versus microbial decomposition on litter chemistry, we also collected spectra from nine samples (n = 3 from each species) that experienced microbial decomposition. Specifically, we took subsamples from the nine litter samples from the control treatment in the above experiment and incubated them with microbial inoculum for one month. Microbial inoculum was made by mixing 30 g of fresh soil from the field site with 1 L of deionized water on a bench shaker for 2 h and then filtering the mixture through a Whatman 40 filter paper to remove soil particles. One gram of litter was placed in a 50-mL plastic beaker with 3 mL of inoculum and loosely covered with laboratory film (Parafilm PM996, Bemis Company, Inc., Neenah, WI) to minimize evaporation. The film cover was periodically removed to avoid

190 excessive accumulation of CO_2 in the headspace. After one month, litter was oven-dried for 2D
191 NMR analysis.

192 All 27 of these samples were evaluated for litter chemical characteristics using 2D ^{1}H–^{13}C
193 heteronuclear single-quantum coherence (HSQC) spectroscopy. The 2D NMR spectra of litter
194 cell wall material were collected following the protocol outlined in Kim and Ralph (2010) and
195 Mansfield et al. (2012). Briefly, litter cell wall material was isolated from litter subsamples using
196 a series of solvent extractions with water, 80% (vol/vol) ethanol, and acetone. The extraction
197 removes soluble compounds that may distort the NMR spectra of litter cell walls. Subsamples of
198 the extracted cell wall material (~250 mg) were finely ground using a ball-mill (Planetary Micro
199 Mill Pulverisette 7 premium line, Fritsch, Idar-Oberstein, Germany). Then, 50 mg of ball-milled
200 cell wall material were swelled in 500 μL of 4:1 dimethylsulfoxide (DMSO-d_6)/pyridine-d_5
201 (vol/vol) to form a gel in a 5-mm NMR tube. The HSQC NMR spectroscopy was performed as
202 described previously (Mansfield et al., 2012) on a Bruker AVANCE 700 Spectrometer (700
203 MHz; Rheinstetten, Germany) with a cryogenically-cooled triple-resonance inverse NMR probe.
204 Central peaks of the DMSO solvent were used as internal reference (δ_H 2.50, δ_C 39.5 ppm).
205 Resonance assignments of lignin syringyl (S), guaiacyl (G), and *p*-hydroxyphenyl (H) units,
206 lignin methoxyl (OMe), the α-position of the lignin β-aryl-ether (A_α), and acetylated xylan units
207 (2-*O*-Ac-β-$_D$-Xyl*p* and 3-*O*-Ac-β-$_D$-Xyl*p*) were confirmed by comparison with previously
208 reported spectra (Ralph et al., 2009; Kim and Ralph, 2010; Talbot et al., 2011; Lan et al., 2015;
209 Lin et al., 2015a). Lignin polymers are composed of S, G, and H monomers that are connected by
210 several inter-unit linkages, including A_α. Acetylated xylan units are key characteristics of
211 hemicelluloses. Relative abundances of A_α, 2-*O*-Ac-β-$_D$-Xyl*p*, and 3-*O*-Ac-β-$_D$-Xyl*p* were
212 estimated by dividing their integrals by the integral of OMe, as OMe has been found to be
213 relatively stable during the early stages of litter decomposition (Lundquist and Lundgren, 1972;
214 Yelle et al., 2013). Relative abundances of lignin S, G, and H units were estimated by calculating

the ratio of each individual integral over the sum of the three integrals. However, high waxes and/or cutin levels in the *Q. douglasii* litter made it impossible to quantify lignin H units because the contours of these structures overlap with each other. Thus we only quantified lignin S and G units of *Q. douglasii.*

Litter degradability. Besides litter chemistry, we also evaluated the biodegradability of litter that had been previously exposed to the UV exposure or control treatments. A subsample (0.25 g) from each of the 18 samples was placed in a 50-mL plastic beaker. Note that this is a separate set of samples from those used for chemical analysis. Microbial inoculum (1.0 mL), which was prepared in the same fashion as described above, was added to each beaker to introduce a uniform group of microbial decomposers. The 50-mL beakers were placed into 473-mL glass jars, sealed, and incubated for 86 days in the dark in the environmental control room described above. Litter biodegradability was estimated by measuring the microbial CO_2 production during the incubation. Every two to four days, 1 mL of headspace was collected using a syringe and needle through a butyl rubber septum on the lid and analyzed for CO_2 concentration using an infrared gas analyzer (LI-COR 6252, LI-COR Corporation, Lincoln, NE). At each sampling date, a four-point calibration curve was built to standardize CO_2 measurements. Microcosm headspace was flushed periodically with a tank of compressed air to prevent the headspace CO_2 concentration from exceeding 1%. On sampling dates when the headspace was not flushed, 1 mL of CO_2-free air was extracted from a column filled with soda lime and injected in each microcosm to balance pressure. Headspace CO_2 content (in μg) was calculated using the ideal gas law under ambient environmental conditions. Microbial CO_2 production was estimated using the net CO_2 accumulation in the headspace. Litter samples also received 1 mL of deionized water approximately every 15 days during the 86-day incubation to account for loss of water through evaporation and headspace venting.

2.3. Short-term photopriming experiment

To assess photopriming on a timescale of days, we established a factorial design with two levels of moisture conditions (wet and dry) and two radiation regimes: alternating between UV exposure and darkness ("alternating" treatment), and continuous darkness ("dark" treatment). We used only *B. diandrus* litter for this experiment. Litter was cut into small pieces of roughly 1 cm length and placed in 473-mL glass jars. Each microcosm received 1.0 g of litter that fully covered the jar bottom without significant overlap. Litter in the wet treatment received 2 mL of microbial inoculum that was prepared as described above, while litter in the dry treatment was kept dry. Glass jars were fitted with lids made of UV-transparent SUVT plastic (0.32 cm thickness, Spartech Polycast, Stamford, CT), which transmits at least 90% of UV radiation, and then sealed with clear silicon caulk (GE5060, General Electric Company, Huntersville, NC). The silicon caulk was allowed to cure overnight before the start of the experiment. A total of 20 microcosms were prepared (n = 5) and half of them received an alternating cycle of UV exposure phase and dark phase. In the UV exposure phase, microcosms were placed 2 cm under a set of four UV lamps for two days in the environmental control room described above. The distance between UV lamps and litter was approximately 16 cm. The UV lamps were pre-burned for five days to stabilize radiation output. In the dark phase, microcosms were moved to a closed cardboard box in the same room for two days. Microcosms in the dark treatment were kept in another closed cardboard box continuously during the whole experiment. Our UV lamps did emit a small amount of visible light that was assumed to have limited effects on litter decomposition. We acknowledge that filtered lamps (i.e. UV radiation was filtered) would have provided a more rigid control than continuous darkness. Two empty microcosms were constructed as blanks and treated as those in the alternating treatment. Radiation intensity was monitored periodically with the broadband radiometer. Half of the lamps were replaced with pre-burned ones at around Day 40 of the experiment.

Every two days, we measured the headspace CO_2 content of all microcosms using the method described above for a total period of 128 days. As is standard practice for litter incubation studies, the CO_2 production rate was expressed based on the initial litter mass because there was no practical way to continuously measure the dry weights of litter samples throughout the incubation. Because of the high CO_2 production rate, the headspace of microcosms in the wet treatment was flushed using a tank of compressed air every two days until Day 60 of the experiment and every four days thereafter. Headspace CO_2 concentration accumulated very slowly in microcosms in the dry treatment, thus flushing was conducted only twice during the entire experiment (Days 78 and 94). To maintain the moisture conditions, the wet treatment received 1 ml of deionized water on five occasions (Days 44, 60, 78, 94, and 114). On Day 12 of the experiment, microcosms received two extra days of UV exposure due to an error; we decided to keep these microcosms in the dark for the next four days to keep the total duration of UV and dark phases equal.

To assess the impacts of UV exposure on temperature, we placed iButton temperature sensors (n = 3 for both the alternating and dark treatments; DS1921, Maxim Integrated, San Jose, CA) at the bottom of empty glass microcosms and sealed them in the same way as described above. These microcosms were exposed to treatments between Day 26 to Day 40. On average, we observed that UV exposure increased air temperature by up to 2 °C. To control for the effects of temperature on decomposition, we raised the temperature of the microcosms in the dark treatment by 2 °C by placing them in a dark, controlled-temperature incubator (Lab-Line Instruments, Dubuque, IA) during the UV phase for Days 94 to 114 of the experiment. During the dark phase, microcosms were removed from the incubator and placed in a cardboard box in the environmental control room. This allowed the alternating and dark treatments to experience the same temperature fluctuations during Days 94 to 114 of the experiment. The effectiveness of the temperature control was confirmed with iButton sensors in two empty microcosms.

289 At the end of the experiment (128 days), litter pieces were carefully taken out of the
290 microcosms using tweezers, placed in aluminum weighing dishes, and oven-dried at 60 °C for
291 two days. Litter dry weight was recorded. A subsample (100 mg) was added to 50 mL deionized
292 water and soaked for 24 h at 4 °C. The leachate was filtered through a glass microfiber filter
293 (Type A/E, Pall Corporation, Port Washington, NY) and then analyzed for dissolved organic C
294 and N concentrations via a Total Organic Carbon/Nitrogen analyzer (Series V, Shimadzu
295 Corporation, Kyoto, Japan) with potassium biphthalate used to build standard curves.

296 2.4. Statistical analyses

297 In the two-phase photopriming experiment, effects of UV exposure on litter mass loss and
298 biodegradability were assessed using T-tests for each of the three species. We chose the T-tests
299 instead of multiple range tests (e.g. the Tukey's test) because we were mainly interested in the
300 UV effects but not the relative differences among three types of litter. Effects of UV exposure
301 and microbial decomposition on the NMR-derived cell wall characteristics were compared using
302 one-way analysis of variance (ANOVA) per species followed by Tukey's tests. In the short-term
303 photopriming experiment, cumulative and instantaneous CO_2 production and dissolved organic C
304 and N concentrations of litter were compared using two-way ANOVAs. T-tests were then used to
305 examine the effects of radiation exposure since ANOVA revealed order-of-magnitude differences
306 between dry and wet treatments. All statistical analyses were conducted in R (R Development
307 Core Team, 2016).

308 **3. Results**

309 3.1 Two-phase photopriming

310 Four months of UV exposure in the laboratory increased the mass loss of the *B. diandrus* and
311 *Q. douglasii* litter by absolute magnitudes of 3.3% and 4.0% compared to the dark control,
312 respectively (Fig. 1a, T-tests, $P = 0.023$ and 0.004, respectively). The UV exposure treatment also

tended to increase the mass loss of *A. fatua*, although this effect was not statistically significant (T-test, $P = 0.274$). Litter in the UV exposure treatment received average radiation levels of 11.5 W m^{-2} and 3.3 W m^{-2} in the UV-B and UV-A ranges, respectively. During the experiment, the amount of UV radiation received by the litter samples (i.e. UV exposure received by both sides of litter envelopes) corresponded to four months of UV radiation (from July to October) measured at Sedgwick Reserve. The UV exposure treatment, however, did not affect litter biodegradability: none of the three types of litter showed differences in cumulative CO_2 production between the UV exposure and control treatments during an incubation with microbial inoculum (Fig. 1b). The peak of instantaneous CO_2 production was temporally delayed under UV exposure compared to the control in all three species (Fig. S1). Once the instantaneous CO_2 production rates stabilized, there was no difference between the UV exposure and control treatments.

After four months of UV exposure, the *B. diandrus* litter still exhibited 2D NMR spectra that were similar to those observed in the control samples (Fig. 2). In contrast, one month of microbial degradation drastically altered the 2D NMR spectra of litter cell walls: microbial degradation strongly reduced the relative signal intensity of the lignin β-aryl ethers (A_α and $A_{\beta\text{-}S}$), which are the dominant type of lignin inter-unit linkages, and reduced acetylated xylans (2-*O*-Ac-β-$_D$-Xyl*p* and 3-*O*-Ac-β-$_D$-Xyl*p*) compared to the reference samples in the aliphatic region. Aromatic signals corresponding to lignin H units and tricin almost disappeared in the microbially degraded samples, and microbial degradation consistently broadened NMR contours, a phenomenon commonly observed in samples that have experienced significant chemical or biological degradation (Samuel et al., 2011; Yelle et al., 2013; Lin et al., 2015a).

Quantification of the NMR spectra further confirmed that one month of microbial decomposition strongly reduced the relative abundances of lignin β-aryl ethers (A_α), acetylated xylans (2-*O*-Ac-β-$_D$-Xyl*p* and 3-*O*-Ac-β-$_D$-Xyl*p*), and lignin H units in *B. diandrus* relative to the control (Fig. 3, Tukey's tests, all $P < 0.05$). The UV exposure, on the contrary, did not influence

abundances of A_α and 3-*O*-Ac-β-$_D$-Xyl*p* in *B. diandrus* and even increased the apparent levels of 2-*O*-Ac-β-$_D$-Xyl*p* and H units in *B. diandrus* relative to the control (Tukey's tests, $P = 0.024$ and 0.031, respectively). In *A. fatua*, microbial incubation also decreased the level of 2-*O*-Ac-β-$_D$-Xyl*p* compared to the control (Tukey's test, $P < 0.001$), whereas UV exposure increased it (Tukey's test, $P = 0.039$). Both UV exposure and microbial treatments also increased lignin H units in *A. fatua* relative to the control (Tukey's tests, $P = 0.019$ and 0.024, respectively). Compared to *B. diandrus* and *A. fatua*, litter chemistry of *Q. douglasii* was less responsive to the UV exposure and microbial treatments. The only statistically significant effect on *Q. douglasii* was that UV exposure increased 3-*O*-Ac-β-$_D$-Xyl*p* relative to control and microbial treatments (Tukey's tests, $P = 0.005$ and 0.006, respectively).

3.2. Short-term photopriming

Mass loss and 128-day cumulative CO_2 production showed similar responses to light regime and moisture treatments. Mass loss was much lower in the dry treatment than in the wet treatment (mean±S.E: 6.8±1.0% versus 43.7±0.6%), but it was not affected by light regime under either dry or wet conditions (data not shown). Cumulative CO_2 production was at least two orders of magnitude lower in the dry treatment than in the wet treatment (Fig. 4a). After accounting for the CO_2 emission from the blanks, which received the same pattern of UV exposure as the alternating treatment, there was no observable difference in CO_2 production from the dry litter between the alternating and the dark treatments. In the wet treatment, there was also no difference in cumulative CO_2 production between the alternating and dark treatments. However, from Day 65 to 128, the alternating treatment increased the cumulative CO_2 production from wet litter by 35% relative to the dark treatment (Fig. 4b, T-test, $P < 0.001$). In the same period, the increases in cumulative CO_2 production induced by the alternating treatment were statistically significant both during the UV exposure phase (15.4 vs. 10.6 mg C g^{-1} litter; T-test, $P < 0.001$) and during the dark phase (15.7 vs. 12.2 mg C g^{-1} litter; T-test, $P = 0.005$). Litter in the UV exposure

363 treatment received approximately 4.1 W m^{-2} and 1.1 W m^{-2} in the UV-B and UV-A ranges,
364 respectively.

365 When the litter was wet, temporal patterns of instantaneous CO_2 production further illustrated
366 how the alternating treatment influenced litter decomposition (Fig. 5). On the first sampling day,
367 the litter CO_2 production rate was higher in the dark than in the alternating treatment (T-test, P =
368 0.021). On the next two sampling days, the CO_2 production rate decreased in the dark treatment,
369 while it increased in the alternating treatment. Between Days 4 and 76, there was no statistical
370 difference in CO_2 production rate between the two light regime treatments, although on multiple
371 occasions (e.g. Days 18, 34, 66, and 68), the alternating treatment tended to have higher CO_2
372 production in the UV phase. After the second event of water addition and between Days 78 and
373 94, the alternating treatment showed elevated litter CO_2 production in the UV phase relative to
374 the dark treatment (T-tests, $P < 0.05$). After Day 98, the alternating treatment showed a
375 consistently higher CO_2 production rate in both the UV and dark phases compared to the dark
376 treatment (T-tests, $P < 0.05$). At the end of the experiment, we found that litter in the alternating
377 treatment had higher dissolved organic C (DOC) concentration than that in the dark treatment
378 when litter was wet (Fig. 4c, T-test, P = 0.072), though there was no difference in DOC
379 concentration between the alternating and dark treatments when litter was dry. Dissolved organic
380 N (DON) concentration of litter was not different between experimental treatments at the end of
381 the incubation (data not shown).

382 **4. Discussion**

383 4.1. Two-phase photopriming

384 Four months of continuous UV exposure induced significant litter mass loss in two out of
385 three species of dry litter (Fig. 1a), suggesting that abiotic photodegradation contributed to litter
386 decomposition. The UV-induced increase in mass loss was around 3-4% over the four-month

period. This result suggests that the non-biological contribution of UV photodegradation to mass loss is small in magnitude, which is consistent with a meta-analysis that assessed the effect of abiotic photodegradation on litter mass loss (Wang et al., 2015). We also observed a small but significant amount of litter mass loss in the dark treatment (4-6%). Although litter was oven-dried prior to the experiment, it might have absorbed moisture from the air during the experiment, which could enable microbial decomposition (Dirks et al., 2010).

Previous studies have reported that UV radiation facilitated subsequent microbial litter decomposition (Foereid et al., 2010; Gaxiola and Armesto, 2015; Wang et al., 2015; Yanni et al., 2015). We did not find significant photopriming effects on the degradability of any of the three litter types after four months of UV exposure (Fig. 1b). This result is consistent with our previous results (Lin et al., 2015b), showing that up to one year of field UV exposure did not increase the biodegradability of *B. diandrus*. Other studies have also reported negligible effects of UV exposure on subsequent microbial decomposition of litter in the laboratory (Brandt et al., 2009; Lambie et al., 2014). We found that UV exposure treatment consistently delayed the peak of instantaneous microbial respiration from all litter types (Fig. S1), suggesting that continuous UV exposure inhibited the colonization and growth of microbes from the inoculum onto the litter material. This negative effect could offset the potential positive effect of UV exposure on litter degradability, resulting in a lack of photopriming. The photopriming effect may also depend on the spectral region of radiation. Austin et al. (2016) found that exposure to UV radiation inhibited subsequent microbial decomposition for a group of woody species, while exposure to visible (blue-green) light increased the microbial degradability of these species. Consistent with these studies, our results indicate that four months of exposure to UV radiation does not necessarily increase litter biodegradability. Our NMR analyses revealed that four months of UV exposure had very limited effects on lignin and hemicellulose in litter cell walls (Figs. 2 and 3), again demonstrating that abiotic UV photodegradation is not necessarily sufficient for altering litter

chemistry or biodegradability. These results also led us to examine whether photopriming might occur on a shorter timescale (e.g. daily or diel).

4.2. Short-term photopriming

Our results show that litter CO_2 production was enhanced by the alternating treatment relative to the dark control when litter was wet (Figs. 4 and 5). We attribute these increases in CO_2 production rates to microbial decomposition, as abiotic UV photodegradation was not effective in inducing significant CO_2 production during this experiment (Fig. 4a). The UV-induced increase in litter decomposition could not be explained by minor temperature differences between the treatments, as the effect persisted even after raising the temperature of the dark treatment between Days 94 to 114. Instead our results indicate strong interactions between abiotic and biotic decomposition mechanisms when they operate in concert on daily, as opposed to monthly, timescales. We observed photopriming effects of UV exposure on microbial decomposition, as the alternating treatment increased litter decomposition relative to the dark treatment even during periods when litter did not receive UV radiation (Fig. 5, after Day 96). It is likely that prior UV exposure in the alternating treatment increased the level of labile substrates available for microbial decomposition. Our DOC results indeed support this mechanism, as the alternating treatment showed higher extractable DOC than the dark treatment when litter was wet (Fig. 4c). Exposure of litter to UV radiation could increase the potential activities of microbial extracellular enzymes in degrading litter substrates such as hemicellulose and lignin (Baker and Allison, 2015) and consequently promote litter decomposition and the accumulation of labile C. Effects of UV exposure on litter chemistry, despite being small in magnitude (Fig. 3), might also provide a positive feedback to microbial decomposition by making litter substrates more accessible to microbial decomposers.

As in the two-phase experiment, we found evidence of UV inhibition effects on microbial respiration, as the peak of CO_2 production rate was delayed in the alternating treatment relative to

437 the dark treatment at the beginning of the experiment (Fig. 5). Similar negative effects of UV
438 exposure have been reported by several photodegradation studies (Smith et al., 2010; Lambie et
439 al., 2014; Lin et al., 2015b). Because our UV lamps were used without diacetate film, litter
440 samples could be exposed to a small amount of UV-C radiation that further amplified these
441 negative effects on microbes. Continuous UV exposure likely enhanced the inhibition effects,
442 resulting in more significant delays of microbial respiration in the two-phase experiment than in
443 the short-term experiment (Figs. 5 and S1). Alternating UV exposure with dark conditions, on the
444 other hand, could provide reoccurring time windows to allow microbial decomposers to recover
445 from the UV inhibition effects. The alternating light regime could thus be the key to minimizing
446 the UV inhibition effects and enabling a synergy between abiotic photodegradation and microbial
447 decomposition. The role of light regime (e.g. continuous versus alternating; different frequencies)
448 in mediating the various effects of UV radiation deserves further attention, as recent modeling
449 work suggests that the UV inhibition effect likely occurs simultaneously with photopriming
450 during litter photodegradation (Adair et al., 2017).

451 The above results illustrate a pathway through which UV photodegradation increases litter
452 microbial decomposition on a temporal scale of days. Gliksman et al. (2016) reported similar
453 short-term dynamics between abiotic and biotic decay processes during the dry season in a
454 Mediterranean shrubland. They found significant mutual enhancement between photodegradation
455 in the day and microbial decomposition at night, suggesting that both photopriming and microbial
456 priming of photodegradation occurred at a diel scale. In their study, litter decomposition was
457 strongly regulated by diel variations in humidity, as litter humidity fluctuated between a low level
458 in the day and a high level at night Gliksman et al. (2016). Litter moisture in our experiment was
459 maintained at a relatively high level by regular addition of water. We found that the magnitude of
460 the UV effects on litter decomposition tended to be amplified by water addition. Water addition
461 likely increased the accessibility of litter substrates to microbial decomposers by mobilizing both

462 microbes and their substrates, and water addition consequently enhanced the positive interaction
463 between photodegradation and microbial decomposition. Thus our results imply that positive
464 interactions between UV photodegradation and microbial decomposition are not limited to arid
465 areas. As discussed earlier, the alternating light regime, rather than the prevailing moisture
466 conditions, is perhaps more important in stimulating photopriming effects.

467 Although the UV lamps used in our experiments did not emit significant visible radiation
468 (Majer and Hideg, 2012), we speculate that short-term photopriming could be triggered by visible
469 light. Recent studies have increasingly recognized the importance of visible light in inducing
470 photodegradation (Day et al., 2015; Austin et al., 2016). Future studies should explore the relative
471 effectiveness of visible versus UV radiation during short-term photorpriming. We also recognize
472 that the alternating treatment did not affect the cumulative CO_2 production of wet litter over the
473 entire experiment (Fig. 4a), as there was no response of microbial respiration to the alternating
474 treatment in the first 74 days of the experiment (Fig. 5). Decomposition of labile substrates,
475 which dominates during the early stages of decomposition, is likely to be controlled by biotic
476 decomposition mechanisms and to be less responsive to photodegradation relative to the
477 decomposition of structural carbohydrates and lignin. It is possible that the facilitation effect of
478 UV radiation on microbial respiration is relatively small in magnitude compared to the gross rate
479 of microbial decomposition early in the experiment (e.g., the first 40 days). It is also possible that
480 the inhibitory effects of UV radiation on microbial activity counteracted the photopriming effects
481 early on during the experiment. Thus photopriming only became significant when the rate of
482 microbial respiration dropped below a critical threshold or when the microbial community
483 became adapted to UV radiation.

484 4.3. Lignin degradation

485 In contrast to our initial hypothesis, microbial decomposition was much more effective than
486 abiotic photodegradation in degrading litter cell walls, particularly targeting lignin β-aryl ethers,

H units, and acetylated xylans in *B. diandrus* (Figs. 2 and 3). Despite the large amount of UV radiation received by litter samples, which corresponded to four months of UV exposure at peak intensity at our field site (July to October), no lignin or hemicellulose feature was degraded by UV exposure in all studied litter species (Fig. 3). These results indicate that continuous UV exposure is not particularly effective in degrading lignin or hemicelluloses, which is also consistent with the negligible or small effects of UV exposure on litter mass loss and CO_2 production (Figs. 1a and 4a). Our findings thus challenge the conventional view that abiotic processes are the primary factor in breaking down lignin and subsequently facilitating microbial decomposition.

Surprisingly, the pattern of changes in NMR spectra induced by microbial decomposition matched nicely with those induced by UV exposure in the field, as reported by our previous study (Lin et al., 2015a). In particular lignin β-aryl ethers, H units, and acetylated xylans in *B. diandrus* were degraded by both one year of UV exposure in the field (Lin et al., 2015a) and microbial decomposition in the laboratory (Figs. 2 and 3). This surprising result suggests that microbial decomposition was ultimately responsible for the UV effects observed in the field. Short-term facilitation could reasonably explain this dominant role of microbial decomposition in degrading lignin. Under field conditions, UV exposure in the day could enhance litter microbial decomposition at night, thus creating short-term facilitation effects on a diel scale.

Together with our past research (Lin et al., 2015a), the new results from the NMR analyses (Figs. 2 and 3) and short-term photopriming experiments (Figs. 4 and 5) indicate that abiotic photodegradation alone does not explain the UV-induced changes in lignin and hemicellulose observed in the field; instead, these changes were likely caused by microbial decomposition that was ‘photoprimed’ by UV radiation. Our results therefore have important implications for interpreting results from previously published studies on litter photodegradation. Most of the previous field studies did not explicitly suppress biotic decomposition (reviewed by King et al.,

2012; Song et al., 2013), thus they could not differentiate the contribution of abiotic photodegradation vs. photopriming to litter decomposition. Therefore, the effects of radiation manipulation on litter decomposition processes observed in these studies should be interpreted as the combined effects of abiotic photodegradation and photopriming, rather than a pure abiotic effect. Together with several recent studies (Wang et al., 2015; Austin et al., 2016; Gliksman et al., 2016), our work further suggests that photopriming should account for a large proportion, if not the majority, of the reported litter mass loss and changes in litter chemistry induced by photodegradation. In order to improve the predictions of decomposition rates and C fluxes, biogeochemical models should preferentially incorporate photopriming mechanisms, particularly on diel or at daily timescales, rather than abiotic processes (e.g., Adair et al., 2017).

Our NMR analyses also reveal that microbial decomposition has species-specific effects on litter chemistry. For instance, microbial decomposition degraded acetylated xylans of two grass litters, *B. diandrus* and *A. fatua*, but did not affect those of a tree leaf, *Q. douglasii* (Fig. 3). As the incubation period lasted only 86 days, these litter samples were probably still in the early stage of decomposition in which labile substrates were primarily being degraded. Differences in the composition of labile substrates and cell wall components among the three species are likely responsible for the observed variations in their responses to microbial decomposition. In addition to these species-specific effects, we also found that UV exposure sometimes slightly increased the relative abundances of certain chemical structures (e.g. 2-*O*-Ac-β-$_{D}$-Xyl*p* in *A. fatua* and *B. diandrus*; Fig. 3b). The exact mechanisms behind these effects are unclear. When quantifying acetylated xylan, we calculated its ratio over the lignin methoxyl (OMe) and assumed that lignin methoxyl remained stable during UV photodegradation and microbial decomposition. It is possible that our assumption was not entirely valid for UV photodegradation, as photochemical reactions might preferentially target OMe relative to the acetylated xylan.

5. Conclusions

Our study showed that four months of exposure to UV radiation led to litter mass loss that was statistically greater than the control, though the changes were small in magnitude. Results of our short-term photopriming experiment further illustrate that the photopriming effect can occur on a timescale of days. An alternating light regime at the timescale of days may be critical for reducing UV inhibition effects on microbes and for creating the synergy between UV radiation and microbial decomposition. Microbial decomposition, rather than abiotic UV photodegradation, explained the UV-induced changes in litter chemistry previously observed in a field experiment. To our knowledge, our results are the first to provide chemical evidence that photopriming is primarily responsible for breaking down lignin and hemicellulose during photodegradation. We propose short-term photopriming as a key mechanism during litter decomposition in a wide range of environmental conditions. The results of our work have strong implications for how photodegradation and microbial processes should be represented in models to accurately predict decomposition and ecosystem C cycling.

Acknowledgements

We thank Tom Tran, Keri Opalk, Kana Yamamoto, and Sarah Liu for assistance in the laboratory and in the field. Josh Schimel, Eric Slessarev, Peter Homyak, Joseph Blankinship, Carla D'Antonio, and Oliver Chadwick provided advice on experimental design and data interpretation. Hoon Kim assisted in the interpretation of NMR spectra. We thank three anonymous reviewers for their comments that improved this manuscript. This project was supported by the National Science Foundation under DEB-0935984 and DEB-1406501 to JK and YL. SK and JR were supported by DOE Great Lakes Bioenergy Research Center (DOE Office of Science BER DE-FC02-07ER64494). YL was supported in part by a Graduate Division Dissertation Fellowship at the University of California, Santa Barbara. The authors declare no competing financial interests.

562

563 **References**

564 Adair, E.C., Parton, W.J., Del Grosso, S.J., Silver, W.L., Harmon, M.E., Hall, S.A., Burke, I.C.,
565 Hart, S.C., 2008. Simple three‐pool model accurately describes patterns of long‐term
566 litter decomposition in diverse climates. Global Change Biology 14, 2636-2660.
567 Adair, E.C., Parton, W.J., King, J.Y., Brandt, L.A., Lin, Y., 2017. Accounting for
568 photodegradation dramatically improves prediction of carbon losses in dryland systems.
569 Ecosphere 8, e01892-e01892.
570 Austin, A.T., Ballaré, C.L., 2010. Dual role of lignin in plant litter decomposition in terrestrial
571 ecosystems. Proceedings of the National Academy of Sciences, USA 107, 2-6.
572 Austin, A.T., Méndez, M.S., Ballaré, C.L., 2016. Photodegradation alleviates the lignin
573 bottleneck for carbon turnover in terrestrial ecosystems. Proceedings of the National
574 Academy of Sciences, 4392–4397.
575 Austin, A.T., Vivanco, L., 2006. Plant litter decomposition in a semi-arid ecosystem controlled
576 by photodegradation. Nature 442, 555-558.
577 Baker, N.R., Allison, S.D., 2015. Ultraviolet photodegradation facilitates microbial litter
578 decomposition in a Mediterranean climate. Ecology 96, 1994-2003.
579 Barnes, P.W., Throop, H.L., Archer, S.R., Breshears, D.D., McCulley, R.L., Tobler, M.A., 2015.
580 Sunlight and soil–litter mixing: drivers of litter decomposition in drylands, Progress in
581 Botany. Springer, pp. 273-302.
582 Berg, B., McClaugherty, C., 2008. Plant litter: decomposition, humus formation, carbon
583 sequestration. Springer-Verlag, Berlin, Heidelberg, Germany.
584 Brandt, L.A., Bohnet, C., King, J.Y., 2009. Photochemically induced carbon dioxide production
585 as a mechanism for carbon loss from plant litter in arid ecosystems. Journal of
586 Geophysical Research-Biogeosciences 114, G02004.
587 Brandt, L.A., King, J.Y., Hobbie, S.E., Milchunas, D.G., Sinsabaugh, R.L., 2010. The role of
588 photodegradation in surface litter decomposition across a grassland ecosystem
589 precipitation gradient. Ecosystems 13, 765-781.
590 Brandt, L.A., King, J.Y., Milchunas, D.G., 2007. Effects of ultraviolet radiation on litter
591 decomposition depend on precipitation and litter chemistry in a shortgrass steppe
592 ecosystem. Global Change Biology 13, 2193-2205.
593 Carvalhais, N., Forkel, M., Khomik, M., Bellarby, J., Jung, M., Migliavacca, M., Mu, M.,
594 Saatchi, S., Santoro, M., Thurner, M., 2014. Global covariation of carbon turnover times
595 with climate in terrestrial ecosystems. Nature 514, 213-217.
596 Coŭteaux, M.-M., Bottner, P., Berg, B., 1995. Litter decomposition, climate and litter quality.
597 Trends in Ecology & Evolution 10, 63-66.
598 Day, T.A., Guénon, R., Ruhland, C.T., 2015. Photodegradation of plant litter in the Sonoran
599 Desert varies by litter type and age. Soil Biology and Biochemistry 89, 109-122.
600 Day, T.A., Zhang, E.T., Ruhland, C.T., 2007. Exposure to solar UV-B radiation accelerates mass
601 and lignin loss of *Larrea tridentata* litter in the Sonoran Desert. Plant Ecology 193, 185-
602 194.
603 Dirks, I., Navon, Y., Kanas, D., Dumbur, R., Grünzweig, J., 2010. Atmospheric water vapor as
604 driver of litter decomposition in Mediterranean shrubland and grassland during rainless
605 seasons. Global Change Biology 16, 2799-2812.
606 Feng, X., Hills, K.M., Simpson, A.J., Whalen, J.K., Simpson, M.J., 2011. The role of
607 biodegradation and photo-oxidation in the transformation of terrigenous organic matter.
608 Organic Geochemistry 42, 262-274.
609 Foereid, B., Bellarby, J., Meier-Augenstein, W., Kemp, H., 2010. Does light exposure make plant
610 litter more degradable? Plant and Soil 333, 275-285.

611 Frouz, J., Cajthaml, T., Mudrák, O., 2011. The effect of lignin photodegradation on
612 decomposability of *Calamagrostis epigeios* grass litter. Biodegradation 22, 1247-1254.
613 Gallo, M.E., Porras-Alfaro, A., Odenbach, K.J., Sinsabaugh, R.L., 2009. Photoacceleration of
614 plant litter decomposition in an arid environment. Soil Biology and Biochemistry 41,
615 1433-1441.
616 Gaxiola, A., Armesto, J.J., 2015. Understanding litter decomposition in semiarid ecosystems:
617 linking leaf traits, UV exposure and rainfall variability. Frontiers in Plant Science 6, 1-9.
618 Gliksman, D., Rey, A., Seligmann, R., Dumbur, R., Sperling, O., Navon, Y., Haenel, S., De
619 Angelis, P., Arnone, J.A., Grünzweig, J.M., 2016. Biotic degradation at night, abiotic
620 degradation at day: positive feedbacks on litter decomposition in drylands. Global
621 Change Biology, doi: 10.1111/gcb.13465.
622 Henry, H.A.L., Brizgys, K., Field, C.B., 2008. Litter decomposition in a California annual
623 grassland: interactions between photodegradation and litter layer thickness. Ecosystems
624 11, 545-554.
625 Huang, G., Zhao, H.M., Li, Y., 2017. Litter decomposition in hyper-arid deserts:
626 Photodegradation is still important. Science of the Total Environment 601-602, 784–792.
627 Kim, H., Ralph, J., 2010. Solution-state 2D NMR of ball-milled plant cell wall gels in DMSO-
628 d_6/pyridine-d_5. Organic & Biomolecular Chemistry 8, 576-591.
629 King, J.Y., Brandt, L.A., Adair, E.C., 2012. Shedding light on plant litter decomposition:
630 advances, implications and new directions in understanding the role of photodegradation.
631 Biogeochemistry 111, 57-81.
632 Kirschbaum, M.U.F., Lambie, S.M., Zhou, H., 2011. No UV enhancement of litter decomposition
633 observed on dry samples under controlled laboratory conditions. Soil Biology and
634 Biochemistry 43, 1300-1307.
635 Lambie, S.M.M., Kirschbaum, M.U.F.U.F., Dando, J., 2014. No photodegradation of litter and
636 humus exposed to UV-B radiation under laboratory conditions: No effect of leaf
637 senescence or drying temperature. Soil Biology and Biochemistry 69, 46-53.
638 Lan, W., Lu, F., Regner, M., Zhu, Y., Rencoret, J., Ralph, S.A., Zakai, U.I., Morreel, K., Boerjan,
639 W., Ralph, J., 2015. Tricin, a flavonoid monomer in monocot lignification. Plant
640 Physiology 167, 1284-1295.
641 Lee, H., Rahn, T., Throop, H., 2012. An accounting of C-based trace gas release during abiotic
642 plant litter degradation. Global Change Biology 18, 1185-1195.
643 Leff, J.W., Fierer, N., 2008. Volatile organic compound (VOC) emissions from soil and litter
644 samples. Soil Biology and Biochemistry 40, 1629-1636.
645 Lin, Y., King, J., 2014. Effects of UV exposure and litter position on decomposition in a
646 California grassland. Ecosystems 17, 158-168.
647 Lin, Y., King, J.Y., Karlen, S.D., Ralph, J., 2015a. Using 2D NMR spectroscopy to assess effects
648 of UV radiation on cell wall chemistry during litter decomposition. Biogeochemistry 125,
649 427-436.
650 Lin, Y., Scarlett, R.D., King, J.Y., 2015b. Effects of UV photodegradation on subsequent
651 microbial decomposition of Bromus diandrus litter. Plant and Soil 395, 263-271.
652 Liu, S., Hu, R., Cai, G., Lin, S., Zhao, J., Li, Y., 2014. The role of UV-B radiation and
653 precipitation on straw decomposition and topsoil C turnover. Soil Biology and
654 Biochemistry 77, 197-202.
655 Lombardozzi, D.L., Bonan, G.B., Smith, N.G., Dukes, J.S., Fisher, R.A., 2015. Temperature
656 acclimation of photosynthesis and respiration: A key uncertainty in the carbon cycle -
657 climate feedback. Geophysical Research Letters 42, 8624-8631.
658 Lundquist, K., Lundgren, R., 1972. Acid degradation of lignin. Acta Chemica Scandinavica 26,
659 2005-2023.

Majer, P., Hideg, É., 2012. Developmental stage is an important factor that determines the antioxidant responses of young and old grapevine leaves under UV irradiation in a greenhouse. Plant Physiology and Biochemistry 50, 15-23.
Mansfield, S.D., Kim, H., Lu, F., Ralph, J., 2012. Whole plant cell wall characterization using solution-state 2D NMR. Nature Protocols 7, 1579-1589.
Melillo, J.M., Aber, J.D., Muratore, J.F., 1982. Nitrogen and lignin control of hardwood leaf litter decomposition dynamics. Ecology 63, 621-626.
Parton, W., Silver, W.L., Burke, I.C., Grassens, L., Harmon, M.E., Currie, W.S., King, J.Y., Adair, E.C., Brandt, L.A., Hart, S.C., 2007. Global-scale similarities in nitrogen release patterns during long-term decomposition. Science 315, 361-364.
Preston, C.M., Trofymow, J.A., 2015. The chemistry of some foliar litters and their sequential proximate analysis fractions. Biogeochemistry 126, 197–209.
R Development Core Team, 2016. R-A language and environment for statistical computing, version 3.3.1. R Foundation for Statistical Computing, Vienna, Austria.
Ralph, S.A., Ralph, J., Landucci, L.L., 2009. NMR database of lignin and cell wall model compounds.
Samuel, R., Foston, M., Jiang, N., Allison, L., Ragauskas, A.J., 2011. Structural changes in switchgrass lignin and hemicelluloses during pretreatments by NMR analysis. Polymer Degradation and Stability 96, 2002-2009.
Schade, G.W., Hofmann, R.-M., Crutzen, P.J., 1999. CO emissions from degrading plant matter. Tellus. Series B: Chemical and Physical Meteorology 51, 889-908.
Schaefer, D., Steinberger, Y., Whitford, W.G., 1985. The failure of nitrogen and lignin control of decomposition in a North American desert. Oecologia 65, 382-386.
Sluiter, J.B., Ruiz, R.O., Scarlata, C.J., Sluiter, A.D., Templeton, D.W., 2010. Compositional analysis of lignocellulosic feedstocks. 1. Review and description of methods. Journal of Agricultural and Food Chemistry 58, 9043-9053.
Smith, M.J., Purves, D.W., Vanderwel, M.C., Lyutsarev, V., Emmott, S., 2013. The climate dependence of the terrestrial carbon cycle, including parameter and structural uncertainties. Biogeosciences 10, 583-606.
Smith, W.K., Gao, W., Steltzer, H., Wallenstein, M.D., Tree, R., Resource, N., State, C., Collins, F., 2010. Moisture availability influences the effect of ultraviolet-B radiation on leaf litter decomposition. Global Change Biology 16, 484-495.
Smith, W.K., Reed, S.C., Cleveland, C.C., Ballantyne, A.P., Anderegg, W.R.L., Wieder, W.R., Liu, Y.Y., Running, S.W., 2016. Large divergence of satellite and Earth system model estimates of global terrestrial CO2 fertilization. Nature Climate Change 6, 306-310.
Song, X., Peng, C., Jiang, H., Zhu, Q., Wang, W., 2013. Direct and indirect effects of UV-B exposure on litter decomposition: a meta-analysis. PloS One 8, e68858.
Talbot, J.M., Yelle, D.J., Nowick, J., Treseder, K.K., 2011. Litter decay rates are determined by lignin chemistry. Biogeochemistry 108, 279-295.
Uselman, S.M., Snyder, K.A., Blank, R.R., Jones, T.J., 2011. UVB exposure does not accelerate rates of litter decomposition in a semi-arid riparian ecosystem. Soil Biology and Biochemistry 43, 1254-1265.
van Asperen, H., Warneke, T., Sabbatini, S., Nicolini, G., Papale, D., Notholt, J., 2015. The role of photo-and thermal degradation for CO_2 and CO fluxes in an arid ecosystem. Biogeosciences 12, 4161-4174.
Wang, J., Liu, L., Wang, X., Chen, Y., 2015. The interaction between abiotic photodegradation and microbial decomposition under ultraviolet radiation. Global Change Biology 21, 2095-2104.
Whelan, M.E., Rhew, R.C., 2014. Carbonyl sulfide produced by abiotic thermal and photodegradation of soil organic matter from wheat field substrate. Journal of Geophysical Research: Biogeosciences 120, 54-62.

711 Wieder, W.R., Cleveland, C.C., Smith, W.K., Todd-Brown, K., 2015. Future productivity and
712 carbon storage limited by terrestrial nutrient availability. Nature Geoscience 8, 441-444.
713 Yanni, S.F., Suddick, E.C., Six, J., 2015. Photodegradation effects on CO_2 emissions from litter
714 and SOM and photo-facilitation of microbial decomposition in a California grassland.
715 Soil Biology and Biochemistry 91, 40-49.
716 Yelle, D.J., Kaparaju, P., Hunt, C.G., Hirth, K., Kim, H., Ralph, J., Felby, C., 2013. Two-
717 Dimensional NMR evidence for cleavage of lignin and xylan substituents in wheat straw
718 through hydrothermal pretreatment and enzymatic hydrolysis. BioEnergy Research 6,
719 211-221.

720

721

Figure Captions

Fig. 1. Effects of four months of UV exposure on (**a**) litter mass loss and (**b**) litter biodegradability, which was estimated by cumulative CO_2 production from litter during 86 days of incubation with microbial inoculum from the two-phase photopriming experiment. Error bars indicate standard errors of means (n = 3). Different letters indicate statistical differences between the control and UV exposure treatment at $\alpha = 0.05$ level (T-tests).

Fig. 2. Representative 2D ^{1}H–^{13}C HSQC NMR spectra of whole-cell-wall gels of *B. diandrus* litter in DMSO-d_6/pyridine-d_5 (4:1, vol:vol) in the aliphatic region (**a**-**c**) and the aromatic region (**d**-**f**). Spectra are aligned to present samples from the following treatments (from L to R): control (a, d), four months of UV degradation (b, e), and one month of microbial degradation (c, f).

Fig. 3. Effects of UV and microbial degradation on the (**a**) lignin β-aryl ether (A_α), (**b**) acetylated xylan (2-*O*-Ac-β-$_D$-Xyl*p*), (**c**) acetylated xylan (3-*O*-Ac-β-$_D$-Xyl*p*), and (**d**) lignin *p*-hydroxyphenyl (H) units of *A. fatua*, *B. diandrus*, and *Q. douglasii* litter. Abundances of A_α, 2-*O*-Ac-β-$_D$-Xyl*p*, and 3-*O*-Ac-β-$_D$-Xyl*p* were calculated by dividing their NMR integrals relative to the integral of lignin methoxyl (OMe). Relative abundance of lignin H units was calculated by dividing its integrals by the sum of integrals of all lignin monomers. NA, levels of lignin H units could not be resolved in the spectra of the *Q. douglasii* litter. Error bars indicate standard errors of means (n = 3). Different letters indicate statistical differences among treatments at $\alpha = 0.05$ level (Tukey's tests).

Fig. 4. Effects of dark and alternating treatments (**a**) on the cumulative CO_2 production in the dry and wet treatments during the 128-day short-term photopriming experiment (log scale), (**b**) on the

cumulative CO_2 production in the wet treatment during Days 1-64 and Days 65-128 of the experiment, and (**c**) on the litter dissolved organic C concentration in the dry and wet treatments at the end of the experiment. Error bars indicate standard errors of means (n = 5). Different letters indicate statistical differences between dark and alternating treatments at α = 0.05 (upper case) and 0.10 (lower case) levels (T-tests). Results in (**a**) have been adjusted against the CO_2 production observed in blanks (n = 2).

Fig. 5. Effects of dark and alternating treatments on the CO_2 production rate in the wet treatment during (**a**) Days 1-64 and (**b**) Days 65-128 of the short-term photopriming experiment. Error bars indicate standard errors of means (n = 5). * indicates statistical differences between treatments at α = 0.05 level (T-tests). Arrows indicate water addition events. Grey panels in the background represent the dark phase in the alternating treatment. Note the difference in the scale of CO_2 production between (**a**) and (**b**).

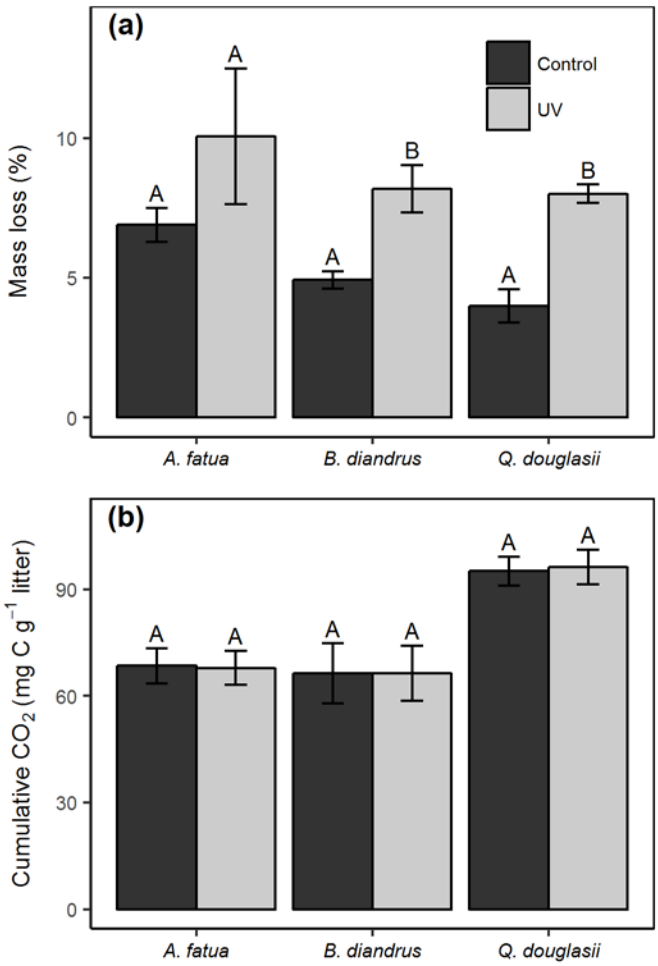
(a)
Control
UV
Mass loss (%)
0
5
10
A
A
B
A
B
A
A. fatua
B. diandrus
Q. douglasii
(b)
Cumulative CO_2 (mg C g^{-1} litter)
0
30
60
90
A
A
A
A
A
A
A. fatua
B. diandrus
Q. douglasii

762

763 Fig.1

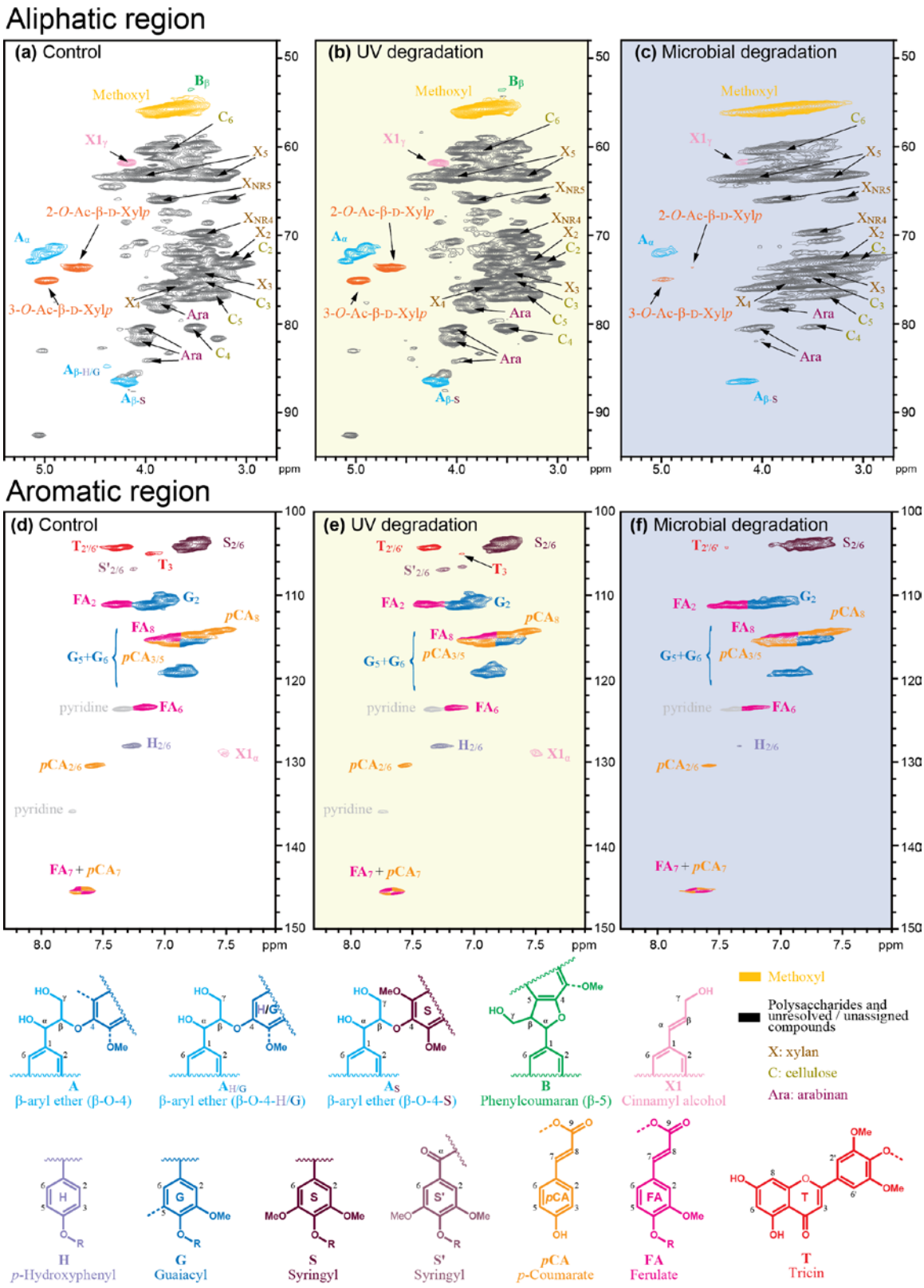

764

765 Fig.2

766 (Color is for the online version only)

767

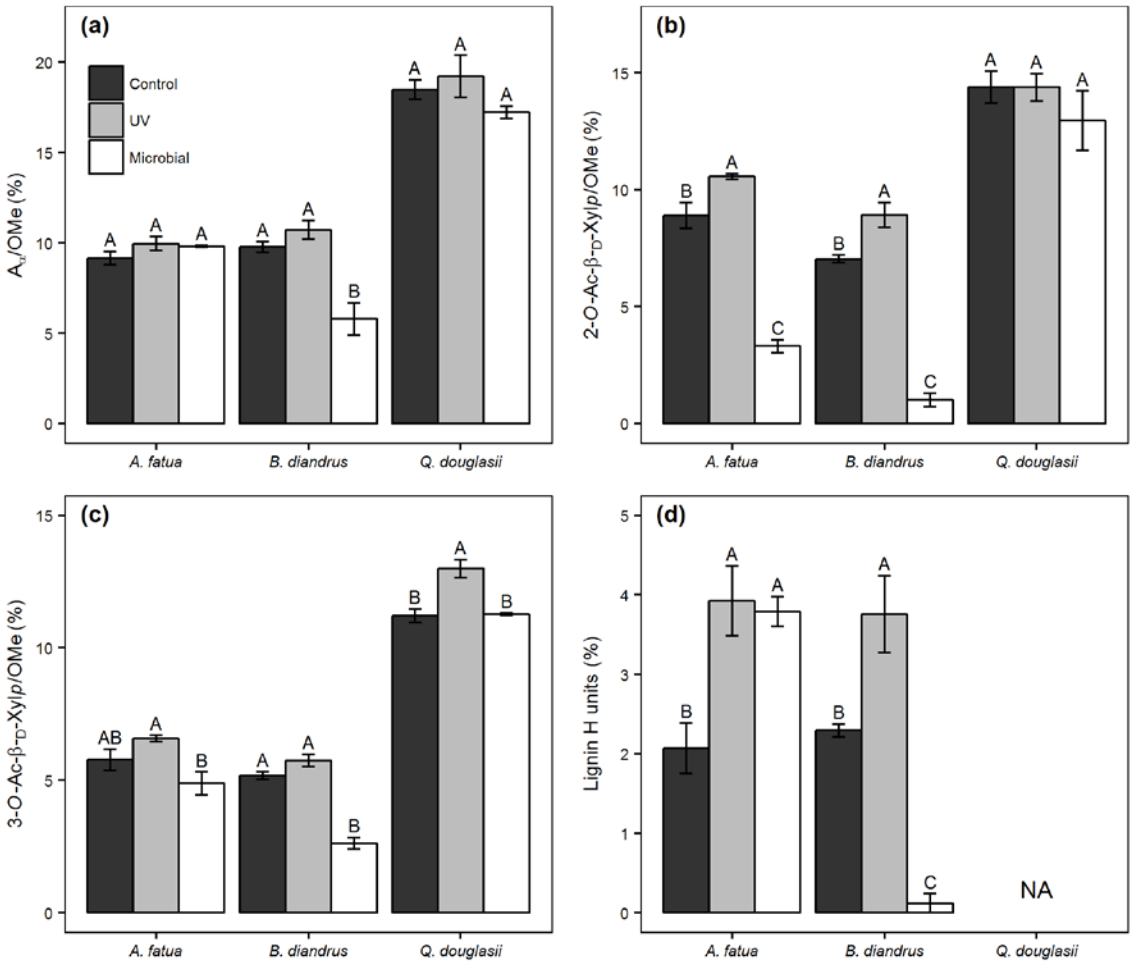

768

769 Fig.3

770

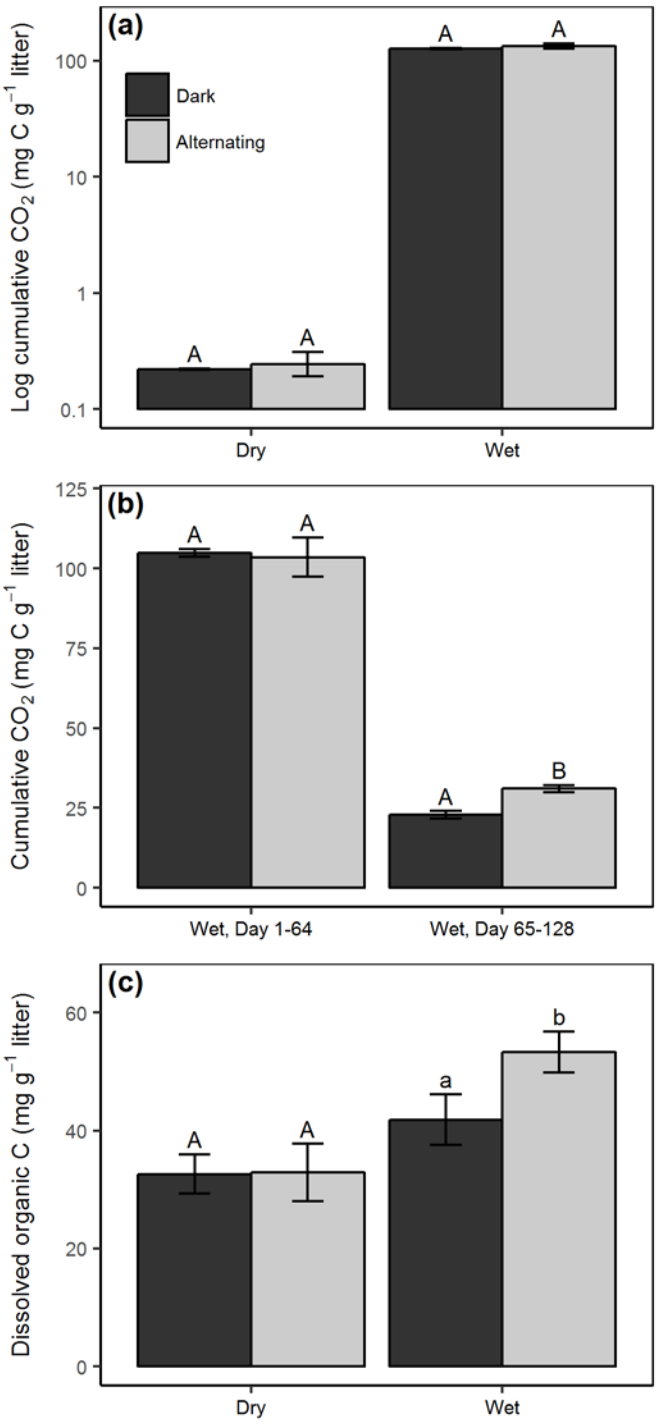
(a)
Dark
Alternating
Log cumulative CO2 (mg C g−1 litter)
100
10
1
0.1
A
A
A
A
Dry
Wet
(b)
Cumulative CO2 (mg C g−1 litter)
125
100
75
50
25
0
A
A
A
B
Wet, Day 1-64
Wet, Day 65-128
(c)
Dissolved organic C (mg g−1 litter)
60
40
20
0
A
A
a
b
Dry
Wet

771

772 Fig. 4

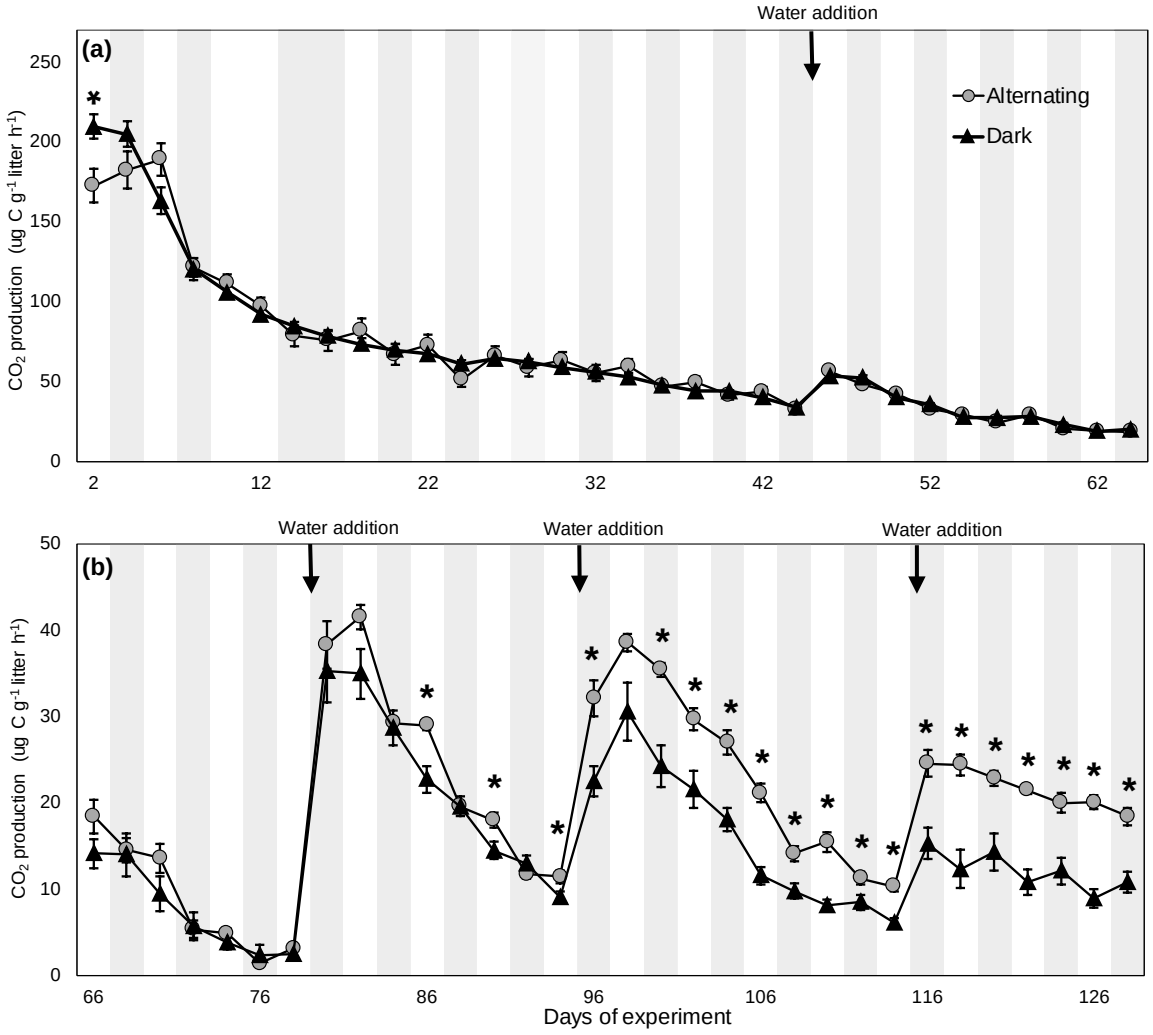
Water addition
(a)
Alternating
Dark
CO_2 production (ug C g^{-1} litter h^{-1})
0
50
100
150
200
250
2
12
22
32
42
52
62
Water addition
Water addition
Water addition
(b)
CO_2 production (ug C g^{-1} litter h^{-1})
0
10
20
30
40
50
66
76
86
96
106
116
126
Days of experiment

773

774 Fig.5

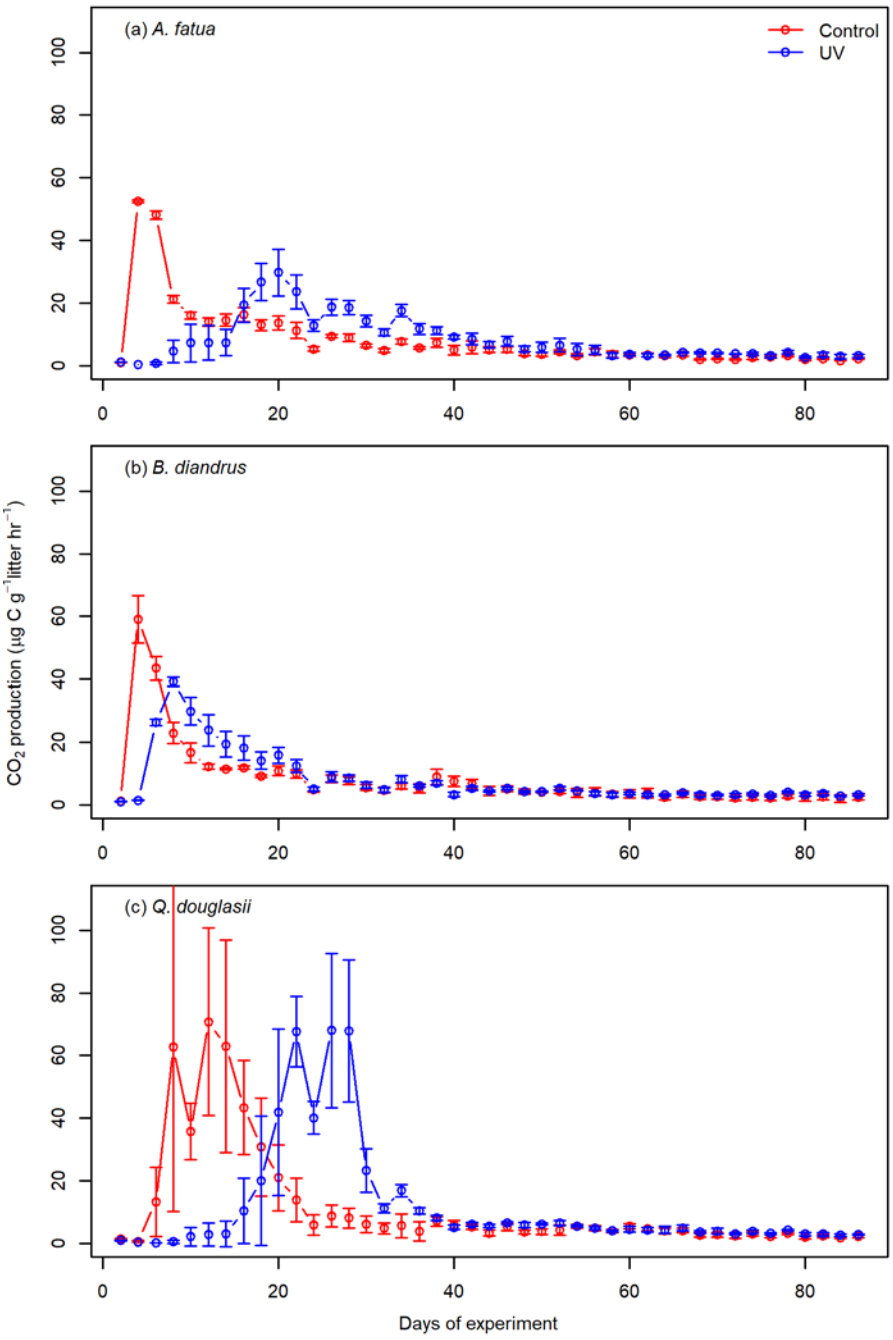

Fig S1. Effects of UV exposure and control treatments on the instantaneous CO_2 production rate of (a) *A. fatua*, (b) *B. diandrus*, and (c) *Q. douglasii* litter during subsequent microbial decomposition. Means and S.E.s are shown.